# Influence of the Monomer Sequential Distribution on the Mechanical Properties and Temperature Dependence of an Ethylene–Tetrafluoroethylene Copolymer in Association with the Phase-Transition Behavior

**Kiyotaka Arai,[1] Atsushi Funaki,[1] Shigeru Aida,[1] Suttinun Phongtamrug,[2] Kohji Tashiro[2]**

[1]*AGC Chemicals, Asahi Glass Company, Limited, Kanagawa, Yokohama 221-8755, Japan*
[2]*Department of Future Industry-Oriented Basic Science and Materials, Toyota Technological Institute, Nagoya 468-8511, Japan*

Received 27 October 2008; accepted 18 February 2009
DOI 10.1002/app.30660
Published online 24 June 2009 in Wiley InterScience (www.interscience.wiley.com).

**ABSTRACT:** The temperature dependence of the mechanical properties of a series of ethylene–tetrafluoroethylene copolymers was interpreted reasonably on the basis of experimental information about the crystalline phase transition and the amorphous-glass transition behaviors. The crystalline phase-transition temperature, the glass-transition temperature, and the bulk modulus were found to depend sensitively on the tetrafluoroethylene content. The magnitude of change in the bulk modulus at the crystalline phase-transition temperature and glass-transition temperature was also found to depend sensitively on the tetrafluoroethylene content. These experimental data were interpreted from various levels, including the distribution of the sequential ratios of ethylene–ethylene, tetrafluoroethylene–tetrafluoroethylene, and ethylene–tetrafluoroethylene segments in the copolymer chains. © 2009 Wiley Periodicals, Inc. J Appl Polym Sci 114: 1710–1716, 2009

**Key words:** glass transition; mechanical properties; structure–property relations

## INTRODUCTION

Ethylene–tetrafluoroethylene copolymer (ETFE) is a melt-processable fluoropolymer with excellent weatherability and thermal and chemical stability.[1] ETFE is used as an insulator for wires and cables, a coating for anticorrosion, and films for greenhouses. This copolymer is known to show a high probability of alternating arrays of ethylene (E) and tetrafluoroethylene (TFE) monomeric units along the chain. The degree of alternation of E and TFE monomer units is dependent on the E/TFE content. Because the physical properties of an alternating copolymer are different in general from those of the corresponding random copolymer, it is important to clarify the properties of ETFEs as a function of E/TFE content because the E/TFE alternation is dependent on the monomer content. In this study, we treated the dynamic mechanical behavior of a series of ETFEs with different contents.

*Correspondence to:* K. Tashiro (ktashiro@toyota-ti.ac.jp).
Contract grant sponsors: Ministry of Education, Culture, Sports, Science, and Technology [through a Collaboration with Local Communities project (2005–2009)].


© 2009 Wiley Periodicals, Inc.

The temperature dependence of the storage modulus ($E'$) has already been reported for ETFE with a 50–80 mol % TFE content, and the four transitions ($\alpha$, $\alpha'$, $\beta$, and $\gamma$) were reported.[2–6] The $\alpha'$ transition was related to the crystalline phase transition, as we mention in a later section.

In the interpretation of dynamic mechanical properties of this copolymer, we need to take into consideration the crystal phase transition between the low- and high-temperature crystal phases.[2–14] Thermal analysis and X-ray diffraction measurement and vibrational spectral measurement have clarified that the crystalline phase-transition temperature ($T_c$) depends on the TFE content sensitively.[6,7,13,14] At the same time, the melting point and glass-transition temperature ($T_g$) were also found to change depending on the TFE content.[6,14]

In this article, we report the temperature dependence of the dynamic viscoelastic properties of the bulk ETFE samples and reveal that the mechanical properties were intimately related with the structural change in the crystalline phase transition and the thermal motion of the chains in the amorphous region. This type of study has never been reported for ETFEs and should give us important information necessary for the interpretation of the physical properties of this copolymer.

**TABLE I**
**Compositions of the ETFE Copolymers Determined by Elemental Analysis**

| | Polymer composition (mol %) | |
|---|---|---|
| No. | TFE | E |
| 1 | 39 | 61 |
| 2 | 50 | 50 |
| 3 | 54 | 46 |
| 4 | 65 | 35 |
| 5 | 71 | 29 |

## EXPERIMENTAL

ETFEs were synthesized by radical polymerization in a fluoro solvent.[15–19] The copolymer composition was determined by elementary analysis for fluorine content. Table I shows the copolymer compositions. As an example, the ETFE with 50 mol % TFE content is called the 50 mol % TFE copolymer in this study.

Unoriented films of 200 μm thick were prepared by compression molding at 300°C followed by quenching in a water-cooled press instrument or by slow cooling to ambient temperature at a rate of 2°C/min. $E'$ and tan δ were measured at 35, 10, and 1 Hz by an IT rheometer (DVA200 IT Co., Ltd., Japan). The heating rate was 2°C/min. The degree of crystallinity ($X$) was evaluated with wide-angle X-ray diffraction (WAXD) data taken with a RINT2500 X-ray diffractometer (Rigaku Co., Ltd., Japan). The temperature dependence of the lattice spacings was measured between −40 and 200°C with a Rigaku RINT/TTR-III diffractometer.

## RESULTS AND DISCUSSION

### $T_c$ and $T_g$

Figure 1 shows the temperature dependence of $E'$ and tan δ (tan $\delta = E'/E'$, where $E''$ is the loss modulus) measured at 35, 10, and 1 Hz for the melt-quenched 50 mol % TFE copolymer sample. There are four transition peaks, α, α′, β, and γ, as already reported.[3,4,6] The α and γ transitions are related to the thermal motions of chains in the amorphous region because the transition temperatures depend on the measurement frequency. The α transition corresponds to the glass transition of the amorphous region. The α′ is assigned to the crystal transition between the low- and high-temperature phases, as reported.[3–10] The broad peak β is also assigned to the structural change in the crystal lattice, but the details are not yet clear.

Figure 2 shows the temperature dependence of $E'$ and tan δ of the 50 mol % TFE copolymer compared between the samples prepared under different conditions. In case of the slowly cooled sample, the α transition temperature or $T_g$ was higher and the peak height of tan δ was lower than those of the quenched sample. The tan δ peaks of the α′ and β transitions were higher and those of the α and γ transitions were lower for the slowly cooled sample. When we took into account the difference in crystallinity between these two samples, the assignments of the α′ and β transitions to the crystalline phase seemed reasonable from these data.

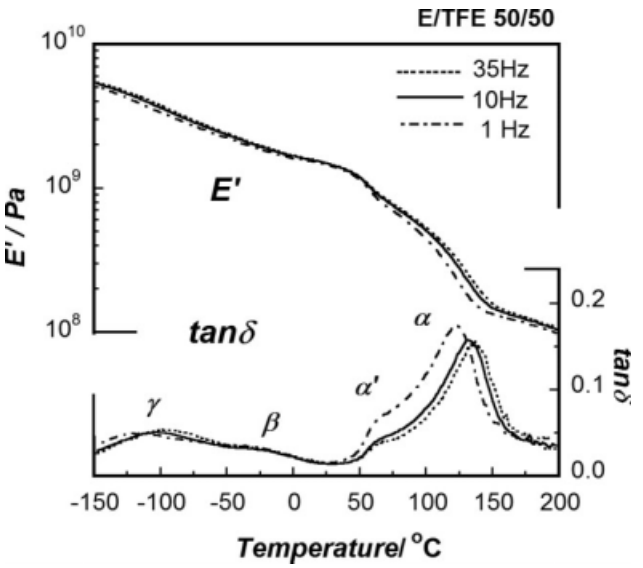


**Figure 1** Temperature dependence of $E'$ and tan δ measured for a melt-quenched sample with 50 mol % TFE copolymer at 35, 10, and 1 Hz.

Figure 3(a–d) shows the temperature dependences of $E'$ and tan δ measured for the ETFEs with TFE 39, 50, 65, and 71 mol % contents, respectively. In these figures, the temperature dependences of the crystal lattice spacings $d$(120) and $d$(200), estimated by the

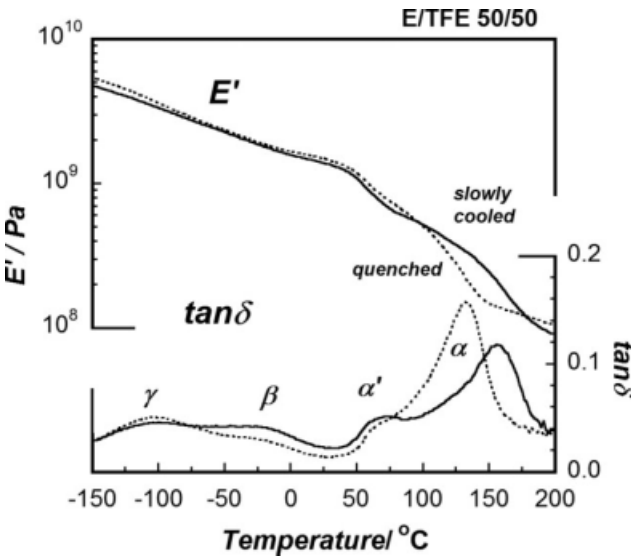


**Figure 2** Comparison of the temperature dependence of $E'$ and tan δ for samples prepared under different conditions with 50 mol % TFE copolymer (frequency = 10 Hz).

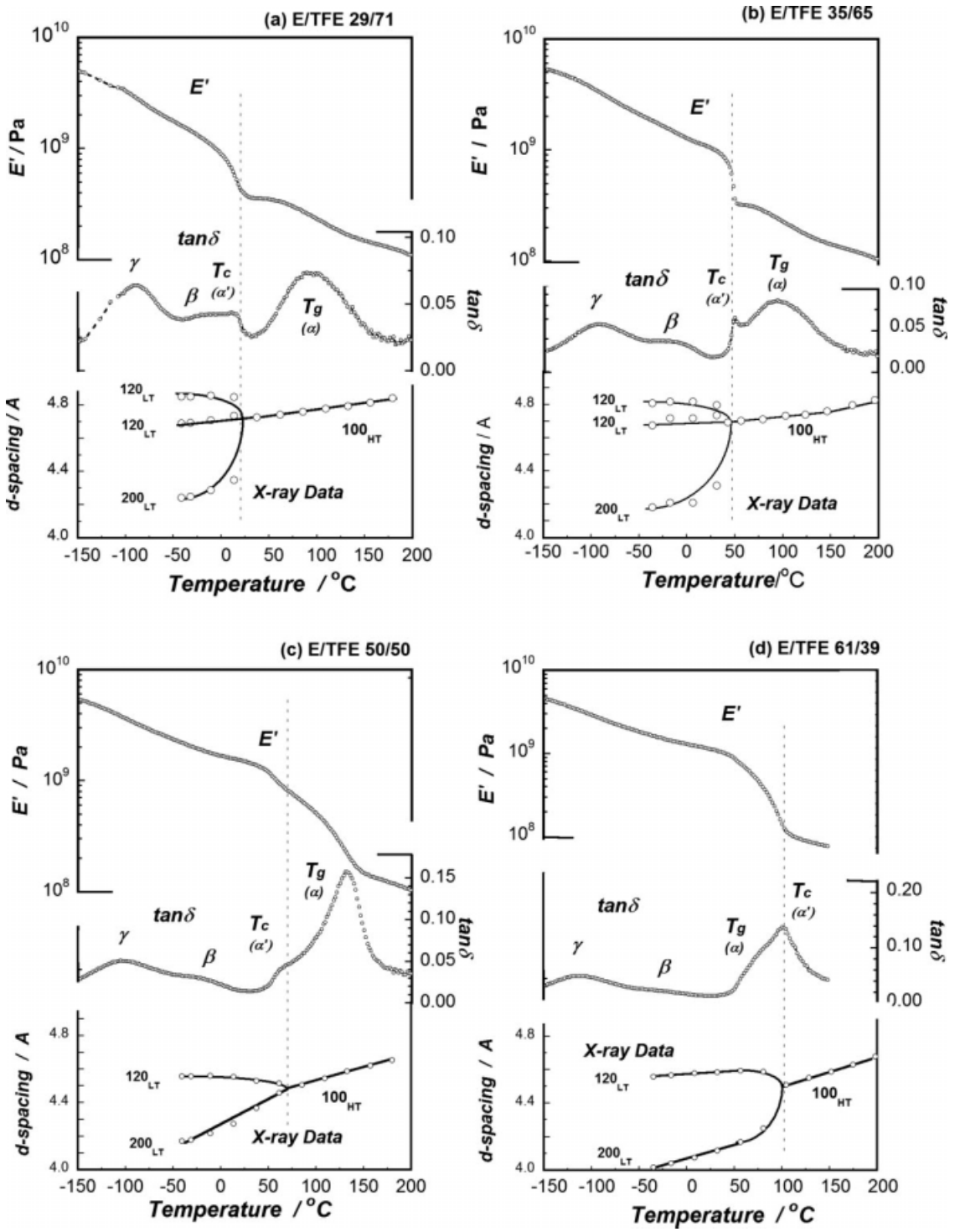


**Figure 3** Temperature dependence of $E'$ and tan δ measured for melt-quenched samples of ETFE with various TFE contents: (a) 71, (b) 65, (c) 50, and (d) 39 mol % (frequency = 10 Hz). LT and HT are the low-temperature and high-temperature phase, respectively.

X-ray diffraction data, are also shown for comparison. The α′ peak position shown in the tan δ curve corresponded well to $T_c$ for all of the samples.

Figure 4 shows the plot of $T_c$ and $T_g$ versus the TFE content. The α peak or $T_g$ was higher than $T_c$ for the copolymers with 50–70 mol % TFE content, whereas the copolymer with 39 mol % TFE showed the crystalline phase transition in a temperature region that was higher than $T_g$.

In this way, $T_g$ and $T_c$ were sensitively dependent on the E/TFE content of the copolymers, and the crossover occurred around the 40 mol % TFE region.

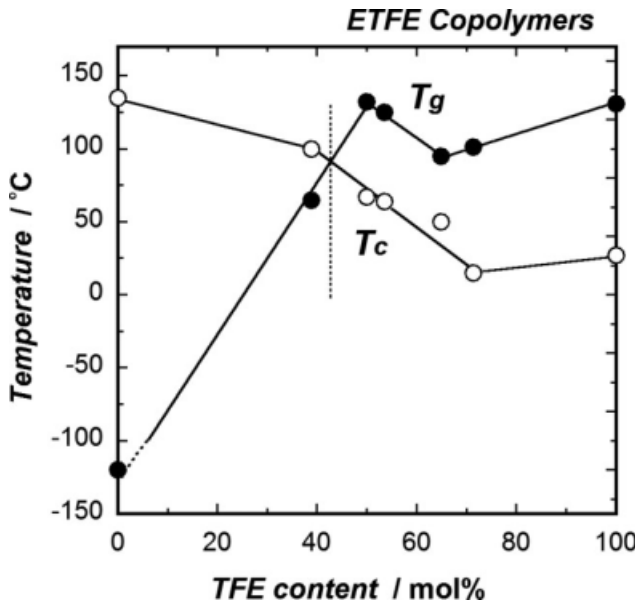


**Figure 4** Influence of the TFE content on $T_c$ and $T_g$ of melt-quenched samples of ETFE (frequency = 10 Hz).

$T_g$ corresponded generally to the temperature region where the micro-Brownian motion of the skeletal chains occurred in the amorphous region through the torsional motions around C—C bonds. Simply said, $T_g$ was governed mainly by the energy barriers for the C—C torsional motion of the amorphous chain. On the other hand, $T_c$ was the temperature where the rotational (or librational) motion of the essentially planar zigzag chains occurred around the chain axis, and the pseudohexagonal packing of these chains was attained as a result. In contrast to the vinylidene fluoride copolymer,[20,21] the chain conformation was almost the trans zigzag form, and the change to gauche form occurred only at a low probability.[13,14] Therefore, the intermolecular interaction energy between the nonbonded H···H, H···F, and F···F atoms were considered to affect the transition temperature significantly. The X-ray structure analysis told us that the unit cell size (the *a* and *b* axial lengths) increased with increasing TFE content.[14] Therefore, the distance between the neighboring chains became longer, and the intermolecular interactions were weaker, which resulted in the easier librational motion of the chains and a remarkable decrease in $T_c$ (as shown in Fig. 4). On the other hand, the ease of torsional motion around the skeletal chains (in the amorphous region) was governed by the local torsional energy barriers around the C—C bonds and was not affected very much by the TFE content; this reflected on the small change in $T_g$. $T_g$ and $T_c$ were, of course, the transition temperatures intrinsic to the amorphous and crystalline regions and were independent each other. Therefore, the crossover of $T_g$ and $T_c$ was only apparent. However, it might be valuable to discuss the reason why such a crossover was observed from the energetic point of view.

Another key point in Figure 4 was the observation of a maximum of $T_g$ for the 50 mol % TFE copolymer. This copolymer had an almost perfect alternating arrangement of E and TFE units along the skeletal chains. As pointed out previously, in the 50 mol % TFE copolymer, it was difficult to change the chain conformation in the phase transition phenomenon because of the overwhelming stability of the trans zigzag form.[14,22]

This suggests that the alternately arranged sequences of E and TFE units showed higher energy barrier for the trans–gauche conformational exchange. This situation may have also been realized for the chains in the amorphous region. The origin of the maximum $T_g$ for the 50 mol % TFE copolymer may have come from such a high rigidity of the alternate copolymer chain. For more detailed and quantitative discussion, we need to perform the molecular dynamics calculation by taking all the energy terms into consideration at the various temperatures.

### Temperature dependence of $E'$ with respect to the crystal phase transition and glass transition

$E'$, measured below $T_c$, showed the maximum for the copolymer with 50 mol % TFE content, as shown in Figure 5. This maximum modulus of an almost perfectly alternating copolymer sample may be interpreted qualitatively on the basis of the rigidity of the molecular chain in the amorphous region.

When the change of $E'$ (and tan δ) occurring in the $T_c$ region was compared among the various copolymers, one remarkable point was noticed. The

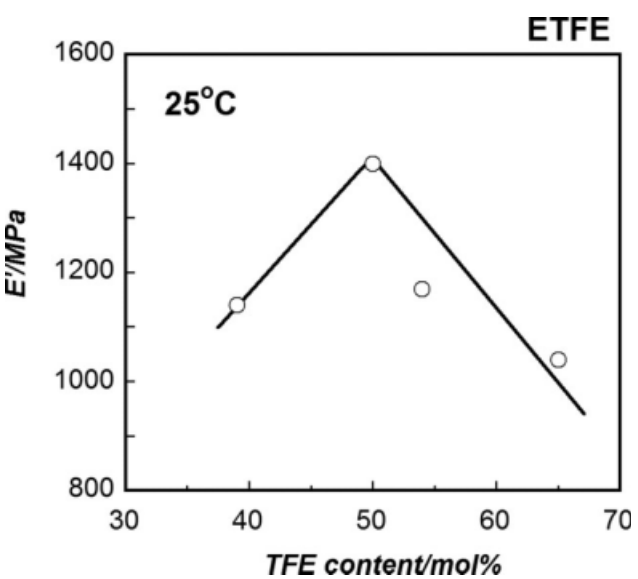


**Figure 5** TFE content dependence of $E'$ for melt-quenched and unoriented ETFE samples measured at room temperature.

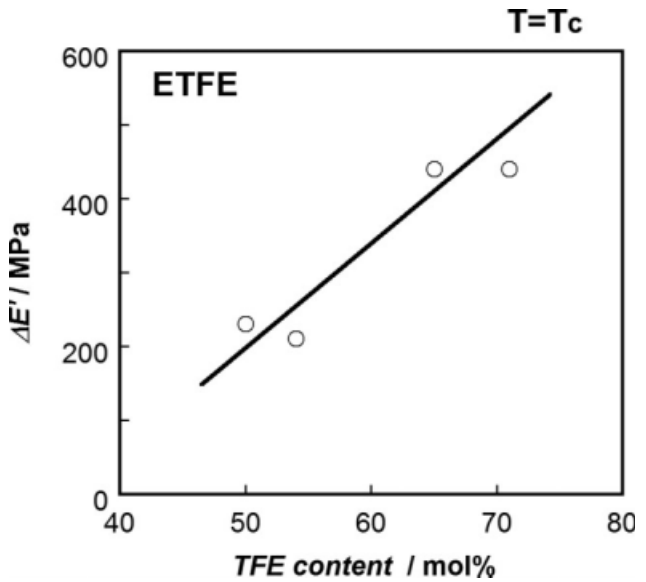


**Figure 6** TFE content dependence of the reduction magnitude of $E'$ at the phase-transition point for unoriented ETFE samples (frequency = 10 Hz).

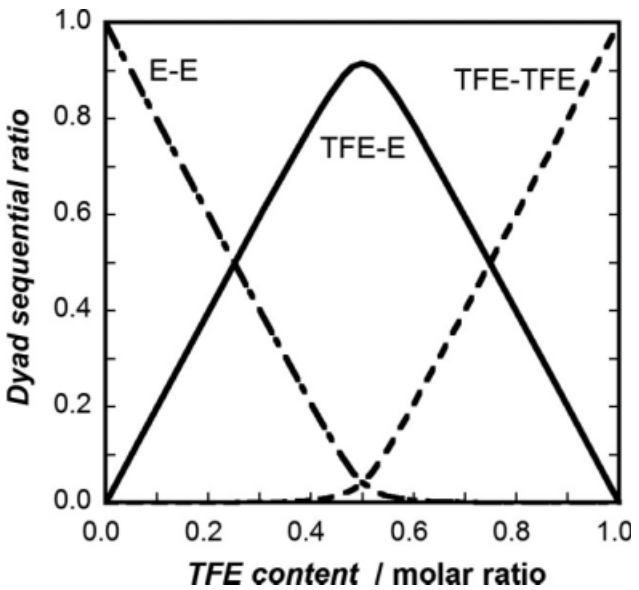


**Figure 7** Dyad sequence ratios calculated for ETFE [the monomer reactivity ratios were 0.06 and 0.14 for TFE (first monomer) and E (second monomer), respectively].

change in the storage modulus ($\Delta E'$) or the magnitude of the $E'$ reduction before and after the phase transition was dependent on the TFE content, as shown in Figure 6. $\Delta E'$ was larger for the copolymer with a higher TFE content.

These changes in $E'$ of the bulk samples were naturally related to the changes in the higher order structure of the crystalline and amorphous phases. These higher order structures and the crystalline state structure was dependent on the chemical regularity of the copolymers. As a result, we can say that the physical properties of these phases were related more or less to the chemical regularity of the copolymer chains or the degree of alternation of the E and TFE units.

When we assumed an ideal copolymerization reaction for this system, the E–E, TFE–TFE, and E–TFE sequential ratios were calculated as shown in Figure 7. The monomer reactivity ratios used for the calculation of the sequential ratios were 0.06 and 0.14 for TFE (first monomer) and E (second monomer), respectively.[18]

In the region of TFE contents of 0.5–1.0, the TFE–TFE and TFE–E sequential ratios were almost linearly in proportion to the TFE content. Therefore, the TFE content dependence of $\Delta E'$ could be redrawn as shown in Figure 8, where $\Delta E'$ is plotted against the TFE–TFE sequential ratio of the copolymer chains. $\Delta E'$ increased in proportion to the increase in the TFE–TFE sequential ratio. This remarkable change in $\Delta E'$ was interpreted as follows. Let us assume here the mechanical series model between the crystalline and amorphous phases as often used in a good approximation. $E'$ is expressed as the bulk modulus ($E_b$) hereafter for clearer expression. $E_b$ may be given as follows:

$$1/E_b = X/E_c + (1 - X)/E_a \quad (1)$$

where $E_c$ and $E_a$ are the moduli of the crystalline and amorphous regions, respectively. If the change in the modulus is small, the following relation is obtained in a good approximation.

$$\Delta E_b = [X/(E_b/E_c)^2]\Delta E_c + [(1 - X)/(E_b/E_a)^2]\Delta E_a \quad (2)$$

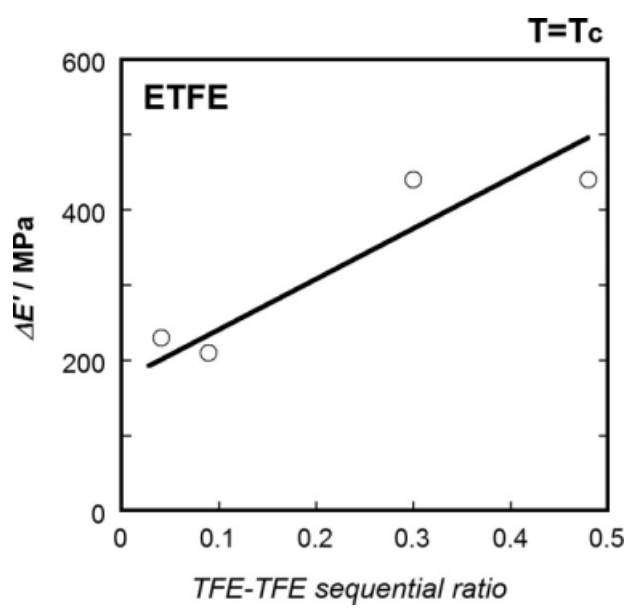


**Figure 8** TFE–TFE sequential ratio dependence of the reduction magnitude of $E'$ measured for unoriented ETFEs at $T_c$.

where $\Delta E_a$ is the change in modulus occurring in the amorphous region at $T_g$, $\Delta E_b$ is the change in the bulk modulus, and $\Delta E_c$ is the change in modulus occurring in the crystalline region at $T_c$. Because the samples used in this study were unoriented, $E_c$ was an isotropic modulus of the crystalline region and could be expressed as the average of the modulus along the chain axis ($E_{\text{chain}}$) and the modulus in the lateral direction ($E_{\text{lateral}}$):

$$3/E_c = 1/E_{\text{chain}} + 2/E_{\text{lateral}} \quad (3)$$

$E_{\text{chain}}$ was much higher than $E_{\text{lateral}}$. Therefore

$$E_c \approx (3/2)E_{\text{lateral}} \quad (4)$$

$E_{\text{lateral}}$ is mainly governed by the intermolecular interactions between the neighboring chains in the crystal lattice and may be in the same order as $E_a$. With eqs. (1) and (4), $E_b$ can be approximately expressed as

$$E_b \approx [3/(3 - X)]E_a \approx E_a(X \ll 1) \quad (5)$$

where $E_{\text{lateral}}$ is substituted by $E_a$. Then, it is reasonable to assume that $E_b \approx E_a \approx E_c$ in a rough estimation. As a result, eq. (2) becomes

$$\Delta E_b \approx X\Delta E_c + (1 - X)\Delta E_a \quad (6)$$

This equation is reasonably understandable in such a point that $\Delta E_b$ is governed by the changes of $E_c$ and $E_a$ in a linear relation.

At the crystalline phase transition point, $T_c$, where the mechanical modulus in the amorphous region is almost not changed or $\Delta E_a \approx 0$, the $\Delta E_b$ is determined almost by $\Delta E_c$ of the crystalline region:

$$\Delta E_b \approx X\Delta E_c \ (\text{at } T_c) \quad (7)$$

On the other hand, $\Delta E_b$ at $T_g$ is governed mainly by $\Delta E_a$ of the amorphous region:

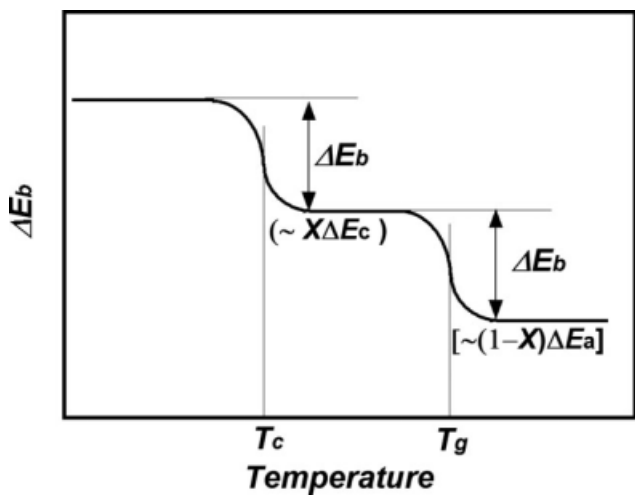


**Figure 9** Schematic illustration of the relation between the reduction of $E'$ and the transitions at $T_c$ and $T_g$.

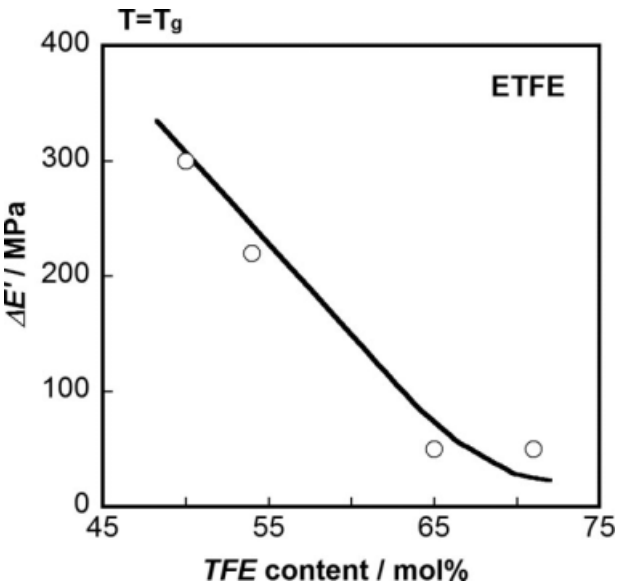


**Figure 10** TFE content dependence of the reduction magnitude of $E'$ measured for unoriented ETFEs at $T_g$.

$$\Delta E_b \approx (1 - X)\Delta E_a \ (\text{at } T_g) \quad (8)$$

In this way, these two types of modulus changes given in eqs. (7) and (8) contribute to $\Delta E_b$ observed at the $\alpha'$ ($T_c$) and $\alpha$ ($T_g$) peaks, respectively, as illustrated in Figure 9.

As shown in Figure 8, $\Delta E'$ (or $\Delta E_b$) at $T_c$ increased as the TFE–TFE sequential ratio was higher. As shown in Figure 3(a–d), the change in the lattice spacing at $T_c$ occurred more remarkably for such a high-TFE copolymer sample. This larger change in the unit cell size resulted in the weaker intermolecular interactions and gave a larger $\Delta E_c$ of the crystalline lattice, which resulted in a larger $\Delta E_b$ at $T_c$, as known from eq. (7). On the other hand, the copolymer with the lower TFE–TFE sequential ratio showed a small change in the chain packing density at $T_c$ because the molecular chains were more slim and packed more strongly, even above the transition point to the pseudohexagonal phase. Then, the change in $\Delta E_c$ was smaller, and $\Delta E'$ (or $\Delta E_b$) was also smaller.

The modulus change $\Delta E_b$ at $T_g$ was also dependent on the TFE content of the copolymer, as shown in Figure 10. The energy barrier of torsional motion around the C—C bonds was higher for the $CF_2$—$CF_2$ bonds than for $CH_2$—$CH_2$ bonds.[20–22] Therefore, the micro-Brownian motion of the amorphous chains was more difficult for the copolymer with a higher TFE content. This means that the change in $E_a$ at $T_g$ was smaller, which resulted in a smaller change in $E_b$, as known by eq. (8).

## CONCLUSIONS

The temperature dependence of $E'$ of ETFEs was related reasonably to $\Delta E_c$ and $\Delta E_a$. Because $\Delta E_c$ and

$\Delta E_a$ were dependent on the TFE content, the magnitude of $\Delta E_b$ was also dependent on the E/TFE content or the sequential ratios of E–E, TFE–TFE, and E–TFE units. As the TFE content was higher, the TFE–TFE sequential ratio was increased, and $\Delta E_b$ became larger. This was interpreted reasonably on the basis of eqs. (7) and (8).

In this way, we related the mechanical property changes of ETFE at $T_c$ and $T_g$ to the changes in the structure and motion of the chains in the crystal and amorphous regions. Of course, we need to clarify the change in the higher order structure or the morphological change to interpret the bulk mechanical properties in a more direct manner. It may be emphasized here that intimate relations could be detected among the chemical structure, the phase transition behavior of the crystal lattice, and the molecular motion in the amorphous region to interpret the temperature dependence of the macroscopic mechanical properties of the ETFE bulk samples.

## References


1. Drobnt, J. Rapra Rev Rep 2006, 16, 184.
2. Starkweather, H. W., Jr. J Polym Sci Polym Phys Ed 1973, 11, 587.
3. Nishimura, H. Rep Res Lab Asahi Glass 1974, 24, 59.
4. Tanigani, T.; Yamaura, S.; Matsuzawa, S.; Ishikawa, M.; Mizoguchi, K. Polymer 1986, 27, 1521.
5. Tanigani, T.; Yamaura, S.; Matsuzawa, S.; Ishikawa, M.; Mizoguchi, K. Polymer 1986, 27, 999.
6. Iuliano, M.; Rosa, D. C.; Guerra, G.; Petraccone, V.; Corrradini, P. Macromol Chem 1989, 190, 827.
7. Aniello, D. C.; Rosa, D. C.; Guerra, G.; Peteraccone, V.; Corradini, P. Polymer 1995, 36, 967.
8. Peteraccone, V.; Rosa, D. C.; Guerra, G.; Luliano, M.; Corradini, P. Polymer 1992, 33, 22.
9. Scheerer, K.; Wilke, W. Colloid Polym Sci 1987, 265, 206.
10. Pieper, T.; Heise, B.; Wilke, W. Polymer 1989, 30, 1768.
11. Rosa, D. C.; Guerra, G.; D'Aniello, C.; Peteraccone, V.; Corradini, P.; Ajroldi, G. J Appl Polym Sci 1995, 56, 271.
12. Phongtamrug, S.; Tashiro, K.; Funaki, A.; Arai, K.; Aida, S. Macromol Symp 2006, 242, 268.
13. Phongtamrug, S.; Tashiro, K.; Funaki, A.; Arai, K.; Aida, S. Polymer 2008, 49, 561.
14. Phongtamrug, S.; Tashiro, K.; Funaki, A.; Arai, K. Polymer 2008, 49, 5072.
15. Tabata, Y.; Shibano, H.; Sobue, H. J Polym Sci 1964, 2, 1977.
16. Modena, M.; Garbuglio, C.; Ragazzini, M. J Polym Sci Polym Lett 1972, 10, 153.
17. Wall, L. A. J Polym Sci Polym Phys Ed 1974, 12, 1303.
18. Miyake, H.; Yamabe, M. Rep Res Lab Asahi Glass 1980, 30, 51.
19. Kostov, G. K.; Nikolov, T. J Appl Polym Sci 1995, 55, 1529.
20. Tashiro, K. Ferroelectric Polymers; Marcel Dekker: New York, 1995; Chapter 2.
21. Lovinger, A. J. Jpn J Appl Phys Suppl 1985, 24, 18.
22. Farmer, B. L.; Lando, J. B. J Macromol Sci Phys 1975, 11, 89.